Geoscience Frontiers 13 (2022) 101352

Contents lists available at ScienceDirect

Geoscience Frontiers

journal homepage: www.elsevier.com/locate/gsf

Research Paper

Seismicity modulation by external stress perturbations in plate boundary vs. stable plate interior

Batakrushna Senapati [a], Bhaskar Kundu [a,*], Shuanggen Jin [b,c]

[a] Department of Earth and Atmospheric Sciences, NIT Rourkela, Rourkela 769008, India
[b] Shanghai Astronomical Observatory, Chinese Academy of Sciences, Shanghai 200030, China
[c] School of Remote Sensing and Geomatics Engineering, Nanjing University of Information Science and Technology, Nanjing 210044, China

ARTICLE INFO

Article history:
Received 19 July 2021
Revised 26 November 2021
Accepted 20 January 2022
Available online 21 January 2022
Handling Editor: C.J. Spencer

Keywords:
Seismicity modulation
Resonance destabilization
Plate boundary
Stable plate interior

ABSTRACT

Characterization of critically stressed seismogenic fault systems in diverse tectonic settings can be used to explore the stress/frictional condition of faults, along with its sensitivity for seismicity modulation by periodic stress perturbation. However, the process of seismicity modulation in response to external stress perturbation remains debated. In this paper, the characteristic difference in the seismicity modulation due to resonance destabilization phenomenon governed by rate-and-state friction is presented and validated with the globally reported cases of seismicity modulation in diverse tectonic settings. The relatively faster-moving plate boundary regions are equally susceptible for both shorter-period (e.g., semi-diurnal, diurnal, and other small tidal constituents) and long-period (e.g., semi-annual, annual, pole tide and pole wobble) seismicity modulation processes in response to stress perturbations from natural harmonic forcing, including tidal, semi-annual, annual, or multi-annual time scales. In contrast, slowly deforming stable plate interior regions and diffuse deformation zones appear to be more sensitive for long-period seismicity modulation of semi-annual, annual, or even multi-annual time scales but less sensitive for short-period seismicity modulation. This finding is also supported by the theoretical model predictions from the resonance destabilization process and worldwide documented natural observations of seismicity modulation in diverse types of tectonic settings.

1. Introduction

The behavior of critically stressed seismogenic fault systems in diverse tectonic settings (e.g., plate boundary, stable plate interiors, or diffuse deformation zones) in response to applied stress perturbations remains a fundamental question (Ader et al., 2014). The limited range of configurations of stress variations (e.g., constantly increasing stress, sudden step-like stress, or harmonic stress perturbations, etc.), its impact on seismogenic fault systems play an important role in the seismicity modulation process (Gross and Kisslinger 1997; Gross and Bürgmann 1998; Ader et al., 2014). Earthquakes are modulated either by the various anthropogenic activity or natural processes (Arvidsson, 1996; Johnston et al., 1998; Cochran et al. 2004; Hainzl et al., 2006; Foulger et al., 2018; Kundu et al., 2019; Scholz et al., 2019). The earthquakes that are induced by the various anthropogenic activity such as erecting tall buildings, coastal engineering, quarrying, extraction of groundwater, excavation of tunnels, enhanced oil recovery, hydrofracturing, gas storage, and carbon sequestration, etc. are referred as Human-induced Earthquake (Foulger et al. 2018). Foulger et al. (2018) reported ~700 cases of induced seismicity for the period of 1868–2016, out of which, 562 cases are reliable. It has been documented that the predominance of induced seismicity for earthquake magnitude less than M2 (i.e., ~88%), about 66% for minor events (M3-3.9), and about insignificant ~0.7% for the major events (M7-7.9). Therefore, the reported HiQuake database indicates the dominance of seismicity modulation explicitly for the smaller magnitude events. Apart from several anthropogenic processes (Kundu et al., 2015; Foulger et al., 2018; Kundu et al., 2019; Schultz et al., 2020; Tiwari et al., 2021), various natural processes can also modulate the spatiotemporal occurrence of earthquakes that added with regional tectonic loading process and subsequent migration or redistribution of crustal fluids. The various natural factors that can capable to modulate the seismicity are tidal loading (Cochran et al. 2004; Wilcock, 2009; Luttrell and Sandwell, 2010; Scholz et al., 2019), surface ice/snow loading (Heki, 2003), glacial isostatic rebound (Arvidsson, 1996;

* Corresponding author.
E-mail address: rilbhaskar@gmail.com (B. Kundu).

https://doi.org/10.1016/j.gsf.2022.101352

Johnston et al. 1998; Talbot, 1999; Wu et al., 1999; Sauber et al., 2000; Stewart et al., 2000; Hampel et al., 2007), heavy precipitation (Hainzl et al., 2006), atmospheric pressure (Kaniuth and Vetter, 2006; Liu et al., 2009), sediment unloading (Calais et al., 2010), seasonal groundwater change (Tiwari et al., 2021), seasonal hydrological loading (Fu and Freymueller, 2012; Fu et al., 2012; Wahr et al., 2013; Chanard et al., 2014; Panda et al., 2018; Panda et al., 2020), pole tide (Shen et al., 2005), pole wobble (Lambert and Sottili, 2019), etc. In fact, such modulation also has been reported predominantly for smaller magnitude events in diverse types of tectonic settings (Sauber et al., 2000; Craig et al., 2017; Johnson et al., 2017; Kundu et al., 2017).

Interestingly, such processes perturb only small amounts of stress on faults (i.e., few Pa to kPa order), but since the fault systems are critically stressed, hence both the natural or anthropogenic activities that perturb stress in the crust can modulate seismicity (Perfettini and Schmittbuhl, 2001; Perfettini et al., 2001). In fact, in the case of seismicity modulation, several terminologies have been reported, e.g., induced, triggered, stimulated, and nuisance earthquakes based on the relative degree of stress perturbation process on the seismogenic fault system (Toksöz and Kehrer, 1972; McGarr et al., 2002; Foulger et al., 2018). Further, it has also been argued that no lower threshold exists for earthquake triggering, as the faulting geometry is random and earthquakes would have equal probabilities of being delayed or triggered (Ziv and Rubin, 2000).

Therefore, the study of seismicity modulation can provide us a unique opportunity to probe into stress/frictional conditions on the fault regime. In fact, characterization of seismicity modulation, associated with non-linear seismogenic fault systems and understanding their inherent non-linear frictional mechanism has become a central theme in terms of objective seismic hazards and scientific discussions (Rice, 1993; Scholz, 1998; Perfettini and Schmittbuhl, 2001; Perfettini et al., 2001; Ader et al., 2014; Foulger et al., 2018; Schultz et al., 2020). Although, seismicity modulation have been documented extensively in diverse kinds of geodynamic settings (Heki, 2003; Shen et al., 2005; Hainzl et al., 2006; Kaniuth and Vetter, 2006; Liu et al., 2009; Thomas et al., 2009; Calais et al., 2010; Thomas et al., 2012; Panda et al., 2018; Lambert and Sottili, 2019; Panda et al., 2020; Tiwari et al., 2021); however, the contrast in seismicity modulation for different types of tectonic domains (i.e., including plate boundary, stable plate interiors, or diffuse deformation zones), remains debated.

In this article, we investigate the characteristic difference in the seismicity modulation process by fault destabilization due to a resonance phenomenon, considering fault interfaces governed by rate-and-state friction (presented in Section 3). Further, we have validated theoretical model prediction (presented in Section 4.1) with the globally reported seismicity modulation in diverse tectonic settings (presented in Section 4.2). Moreover, to understand the difference in seismicity modulation, it is important to highlight the contrast in seismogenic fault systems in terms of crustal-deformation style and earthquake occurrences process in the plate boundary and stable plate interior domain, respectively (presented in Section 2).

2. Seismogenic fault systems: plate boundary vs. stable plate interior

The plate tectonic paradigm is the driving catalyst to describe the plate motion (Thatcher, 2007), lithospheric deformation (Cooper et al., 2017), diversity in terrestrial landscapes (Ramkumar et al., 2016, 2017; Pal et al., 2018; Panda et al., 2019), earthquake cycle and occurrence of giant mega-thrust to slow-slip earthquakes (Foster et al., 2013; Johnson et al., 2013; Obara and Kato, 2016). In fact, all of the processes are associated with the relatively faster moving plate motion (~10 mm/yr or more) and concentrated deformation along the narrow plate boundaries (Fig. 1a). However, the occurrence of great to moderate magnitude earthquakes within stable plate interior regions also indicates significant amounts of elastic strain that can be released on geological structures far away from the narrow plate boundary faults (Fig. 1a) (Calais et al., 2016). Moreover, earthquakes in the stable plate interior regions represent specific spatiotemporal patterns that certainly differ from those plate boundaries and are associated within the regions where tectonic loading rates are insignificant (Fig. 1b,c) (Mahesh et al., 2012a,b; Calais et al., 2016).

Concept of earthquake cycle (i.e., inter-seismic, nucleation, co-seismic, post-seismic phases), recurrence time, and fault slip-rate well applicable for plate boundary deformation and stable plate interior domain. However, the recurrence intervals of earthquakes in the stable plate interior domain are serval folds larger than the plate boundary domain (Sieh, 1984; Scholz et al., 1986). Generally, the recurrence intervals of earthquakes in the stable plate interior domain are several thousand to tens of thousands of years, whereas recurrence intervals of earthquakes in the plate boundary region are a few hundreds of years (Sieh, 1984; Scholz et al., 1986; Landgraf et al., 2016). The longer recurrence interval in the stable plate interior domain earthquakes than plate boundary earthquakes may possibly due to the low strain accumulation rates (Katsube et al., 2017; Kondo and Owen, 2013). For example, New Madrid Seismic zone, USA, is a well monitoring plate interior domain, having an earthquakes recurrence interval of >1000 years (Schweig and Ellis, 1994). It is also consistent for the regions Meers, Oklahoma (>250 ka, Crone et al., 2003) and Gofukuji fault, Japan (700–1000 years; Okumura, 2001), etc. Moreover, several mechanisms have been proposed to explain the earthquakes occurrence process in the stable plate interior. It includes lithospheric flexure (Bilham et al., 2003), deformation associated with stable continental (and failed rift) region by fault reactivation process (Sykes, 1978), stress/strain localization (Campbell, 1978; Zoback et al., 1985); gravitational induced stress concentration at structural boundaries (Pollitz et al., 2001); reduction of mechanical/-chemical strength by fluid activity (Talwani and Acree, 1985; Costain et al., 1987), etc. However, all the above mechanism persists over long geologic time intervals and probably change the stress field of a stable plate interior domain, but seismicity in the stable plate interior domain does not exist over a long geologic time interval (Calais et al., 2016). Further, it has been argued that the rate of aftershock decay is significantly faster for plate boundary, while the decay rate is slower in the case of stable plate interior domain and overall background stress rate is high in plate boundary in contrast to stable plate interior domain (Fig. 1d) (Stein and Liu, 2009).

Moreover, it has also been argued that the earthquakes associated with the stable plate interior domains are well explained by transient perturbations of local stress or by slow and localized tectonic stress on the long-lived seismogenic faults (Fig. 1e) (Calais et al., 2016). In other words, in the stable plate interior regions, the tectonic stress accumulation rate is very slow, and earthquakes occur as a result of fault strength change or due to external perturbations caused by hydrological loading or unloading or change in pore-fluid pressure (marked by a cyan line in Fig. 1e) (Calais et al., 2016). For instance, elastic stress change of the crust due to melting of large ice sheets (Arvidsson, 1996), loading or unloading of surface and groundwater (Bollinger et al., 2007; Bettinelli et al., 2008; González et al., 2012), etc. may lead to triggering of earthquakes. Moreover, increasing geophysical investigations have sometimes posed challenges to plate tectonics' paradigm, and in fact, now it appears that some boundaries in both oceanic and continental settings are diffuse, with deformation extending over

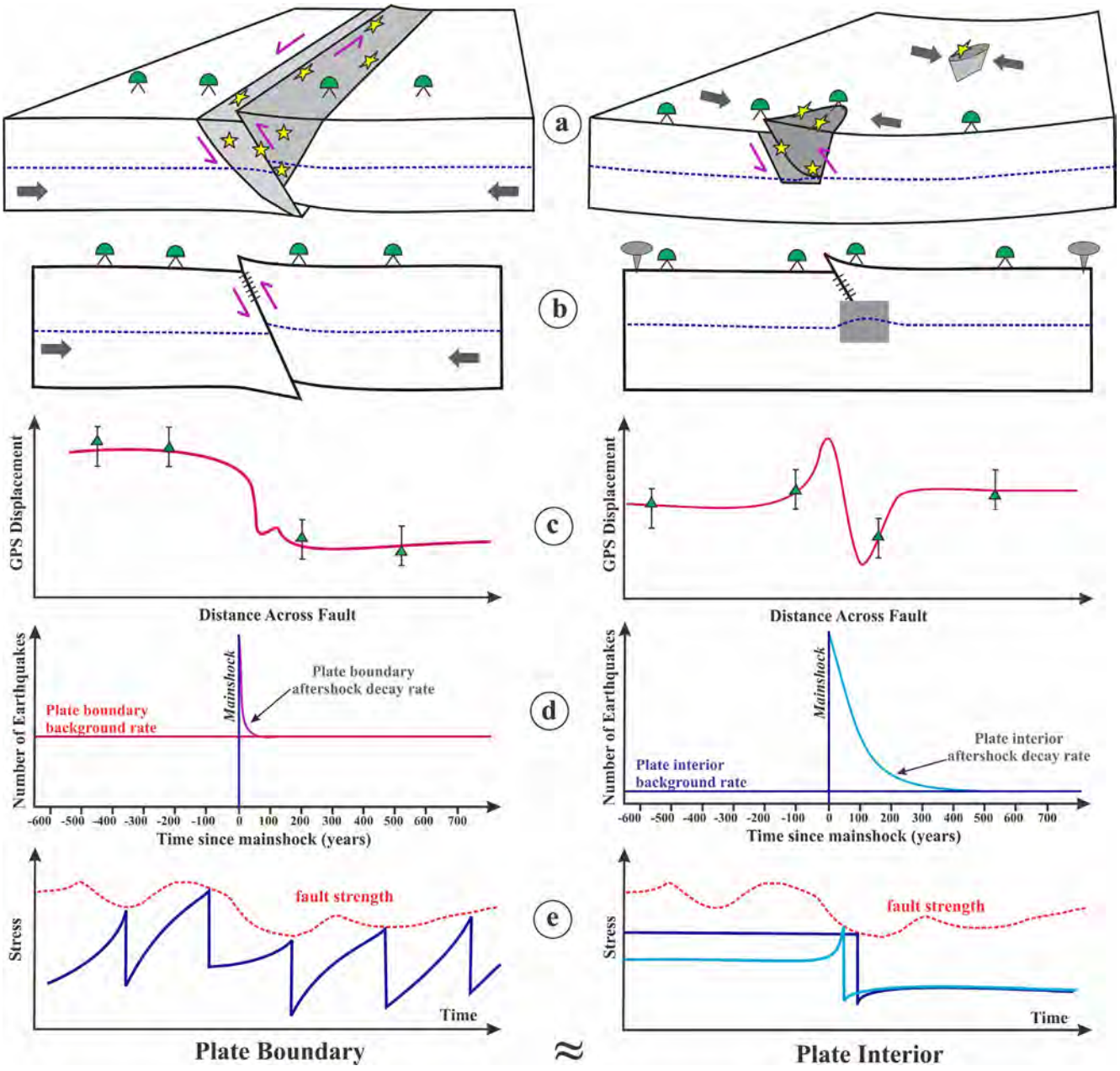

Fig. 1. Schematic representation of the difference in plate boundary vs. stable plate interior deformation styles (a), strain build-up process (b), the reflection of strain build-up process on the gradient in GPS displacement (represented by green symbols) (c), the contrast in Aftershock sequence (d) earthquake occurrence process and subsequent stress change (e) Contrast in stress changes and earthquake sequence in plate boundary and plate interior (adopted from (Mazzotti, 2007; Stein and Liu, 2009; Calais et al., 2016). Blue and Cyan lines are represented by the pore fluid pressure increase at seismogenic depth and hydrological or sedimentary load change with time, respectively. A detailed explanation has been provided in the text (Section 2).

a larger spatial domain, several hundred or even thousands of kilometers wide into plate interior regions (Royer and Gordon, 1997; Zatman et al., 2001). However, a detailed study is required to understand the seismicity modulation process along seismogenic faults in diverse tectonic settings (i.e., plate boundary, stable plate interior, and diffused deformation boundary) and its stress/frictional condition.

3. Theory: Resonance destabilization model

Theoretically (Perfettini and Schmittbuhl, 2001; Perfettini et al., 2001), under laboratory-based conditions (Boettcher and Marone, 2004) and natural case studies (Lowry, 2006; Panda et al., 2018; Panda et al., 2020), it has been established that a small variation in external stress perturbation may destabilize the seismogenic fault systems and enter into a stick–slip domain. Further, a recent study reinvestigated the resonance destabilization process under rate-and-state friction formalism, with a critical emphasis on various physical parameters in diverse tectonic settings, including stable plate interior and plate boundary regions (Senapati et al., 2021). Considering a spring-block model, incorporated with rate-and-state dependent friction law (Fig. S1), Perfettini, (2000) has proposed that the velocity V in response to an oscillatory (or harmonic) stress perturbation of period T and amplitude τ_1 in shear stress and σ_1 in normal stress can be expressed by Eq. (1) (see Supplementary data Text S1 for derivation):

$$\left.\begin{aligned} V &= V_L + Im[V_1 exp(i\omega t)] \\ V_1 &= \rho v exp(-i\gamma v) \end{aligned}\right\} \quad (1)$$

where V_L is the long-term velocity, *Im* means imaginary part and $\omega = \frac{2\pi}{T}$. The parameters ρv and γv are given by Eq. (2):

$$\left.\begin{aligned} \rho v &= \frac{V_L q \tau_{ss}}{k d_c} \sqrt{\frac{E^2+F^2}{C^2+D^2}} \\ tan(\gamma v) &= \frac{DE-FC}{EC-DF} \end{aligned}\right\} \quad (2)$$

Along with Eq. (3)

$$\left.\begin{aligned} C &= 1 - \frac{q^2}{k} \\ D &= q\left(1 - \frac{1}{k}\right) \\ E &= q\left[\epsilon_\sigma\left(1 - \frac{\alpha}{\mu_{ss}}\right) - \epsilon_\tau\right] \\ F &= \epsilon_\sigma - \epsilon_\tau \end{aligned}\right\} \quad (3)$$

Using the variable Eq. (4)

$$\left.\begin{aligned} q &= \frac{V_L}{d_c}\frac{2\pi}{T} \\ k &= \frac{k}{k_c} \\ q &= \frac{q}{q_c} \end{aligned}\right\} \quad (4)$$

and considering the parameters in Eq. (5)

$$\left.\begin{aligned} k_c &= \frac{(b-a)\sigma_*}{d_c} \\ q_c &= \sqrt{\frac{b-a}{a}} \\ T_c &= 2\pi\sqrt{\frac{a}{b-a}}\frac{d_c}{V_L} \\ \mu_{ss} &= \mu_* + (a-b)log\left(\frac{V_L}{V_*}\right) \\ \tau_{ss} &= \mu_{ss}\sigma_* \\ \epsilon_\sigma &= \frac{\sigma_1}{\sigma_*} \\ \epsilon_\tau &= \frac{\tau_1}{\tau_{ss}} \end{aligned}\right\} \quad (5)$$

where τ_{ss} is the steady-state shear stress,μ_{ss} is the steady-state frictional coefficient, d_c is the critical slip distance, a and b are rate-state-dependent frictional parameters,σ_* is the effective normal stress, μ_* is the frictional coefficient. V_* is the reference velocity, τ_1 is the external shear stress and σ_1 is the external normal stress applied to the system, q is the non-dimensional frequency, k_c is the critical stiffness, k is the stiffness of the slipping patch, α is the Linker and Dieterich constant (Perfettini et al., 2001), T is the period of the external perturbation and T_c is the critical period of the external perturbation.

In fact, when we implement the model, the following parameters are known a priori: T, V_L, σ_1, τ_1 and k. Indeed, the long-term velocity V_L is known. The period T of the external perturbation is known and the amplitude of the resulting stress changes σ_1 and τ_1 evaluated on the fault plane can be reasonably estimated. If the dimension of the slipping zone is R, then the corresponding stiffness is of the order of Eq. (6)

$$k = \frac{\gamma G}{R} \quad (6)$$

where G is the shear modulus, R is the dimension of slipping patch and $\gamma = \frac{7\pi}{16}$ for circular cracks (Eshelby, 1957). The parameters that remain unknown are a, b, d_c, σ_*, μ_* and α. Moreover, it is important to note that in rate-and-state friction, the parameters a and b always appear multiplied by the normal stress so that they cannot be derived independently from σ_*. The parameter that accounts for the normal stress changes on the friction coefficient can be neglected (α = 0) or set to the value $\alpha = \frac{\mu_{ss}}{3}$ (Perfettini and Molinari, 2017). Therefore, significant resonance amplification only occurs when the denominator of Eq. (2) is close to 0 and this quantity is independent of the parameter α. Therefore, the parameter α is not relevant when considering strong resonance amplification. As a result, the proposed model essentially depends on the following parameters in Eq. (7):

$$\left.\begin{aligned} \varepsilon &= \frac{b-a}{a} \\ A &= a\sigma_* \\ d_c, \epsilon_\sigma, \epsilon_\tau & \end{aligned}\right\} \quad (7)$$

where ε is the ratio of the difference between the frictional parameters b and a and frictional parameter a, A is the normalized lithostatic pressure,d_c is the critical slip distance,ϵ_σ is the ratio of external normal stress to effective normal stress and ϵ_τ is the ratio of external shear stress to steady-state shear stress. Further, to quantify the physical parameters of the resonance destabilization model, the common practice, the resonance phenomenon will be efficient when $k \approx k_c$ and $T \approx T_c$. Using Eq. (5) together with Eqs. (6) and (7), we have the Eq. (8):

$$\left.\begin{aligned} T_c &\approx \frac{2\pi}{\sqrt{\epsilon}}\frac{d_c}{V_L} \\ R_c &\approx \frac{\gamma G}{A\varepsilon} d_c \end{aligned}\right\} \quad (8)$$

where R_c is the dimension of the patch of critical stiffness k_c (or nucleation size, e.g., Rice, 1993) and must be seen as the characteristic size of the resonating area. So, we look for the set of parameters (A, ε, d_c) that verify Eq. (8). When applying the model to natural/theoretical observations, three unknown parameters have to be inferred, assuming the values $T \approx T_c$ and $R \approx R_c$ given by the observations making the solutions not unique. Introducing the phase lag is not of interest as it would imply introducing two additional parameters (ϵ_σ and ϵ_τ) to the problem, making the problem even more undetermined.

Therefore, to characterize the resonance destabilization process, the three parameters to be inverted are ε, d_c, and A. Their values are constrained by the two important parameters T and R, the period of the forcing term and the size of the resonating region, respectively. The other constants of the model are $\gamma = \frac{7\pi}{16}$ and shear modulus, G, which has considered as 30 GPa. We allow parameter A to span a large range of permissible values, varying from 10^{-9} ρgZ Pa to ρgZ Pa, considering the density of the crustal rock (ρ) 3000 kg/m^3, gravity (g) as 9.8 m/s^2. For each value of A, the parameters ε and d_c are found by minimizing the cost function C, which can be expressed by Eq. (9):

$$C = \sqrt{\frac{\left(1 - \frac{T_c}{T}\right)^2 + \left(1 - \frac{R_c}{R}\right)^2}{2}} \quad (9)$$

The cost function (C) has minimized using MATLAB's routine fminsearchbnd (https://fr.mathworks.com/matlabcentral/fileexchange/8277-fminsearchbnd-fminsearchcon) with d_c being allowed to vary from 10^{-6} m to 0.1 m and ε from 10^{-5} to 10. We have implemented this resonance destabilization model under rate-and-state frictional formalism, to address the contrast of seismicity modulation between plate boundary and stable plate interior's domain associated seismogenic faults system in response to periodic stress perturbations. The above derivation related to the fault resonance model has been presented in the supporting documents.

4. Results

4.1. Theoretical model predictions for seismicity modulation

To present theoretical model predictions and their contrast in seismicity modulation in diverse tectonic settings, under the rate-and-state friction-dependent resonance destabilization (as

described in Section 3), some physical parameters play an important role. Those physical parameters are long-term plate motion velocity in diverse types of tectonic settings (V_L), specific periods for modulation (T), length of the modulating fault patch or dimension of the slipping zone (R), and depth range of the modulation in the crust (Z). In Figs. 2, 4, and 6, we have systematically varied V_L, T, R, and Z, under the realistic ranges of those physical parameters. We considered long-term plate motion velocity (V_L) ranges from 10^{-1} to 10^{2} mm/yr, which covers the overall entire global range of plate motion velocity (or tectonic loading rate of the seismogenic faults) in a diverse types of tectonic settings. According to the classification of tectonic settings (Gordon, 1998; Zatman et al., 2001), we have considered stable plate interior domains (V_L = 0.01–2 mm/yr), diffuse deformation boundary (V_L = 2–16 m m/yr) and relatively faster-moving plate boundary (V_L = 12–100 mm/yr) depending upon variation in long-term plate motion velocity. We considered time periods for modulation (T) ranging from 10^{-3} to 10 years that include all different types of exogenous harmonic stress perturbations process. It includes all tidal (i.e, semidiurnal, diurnal and fortnight constituents), semi-annual (T = 6 months), annual (T = 1 yr), pole tide (T = 14 months) and pole wobble frequency (T = 6.4 yr). These are the only natural harmonic

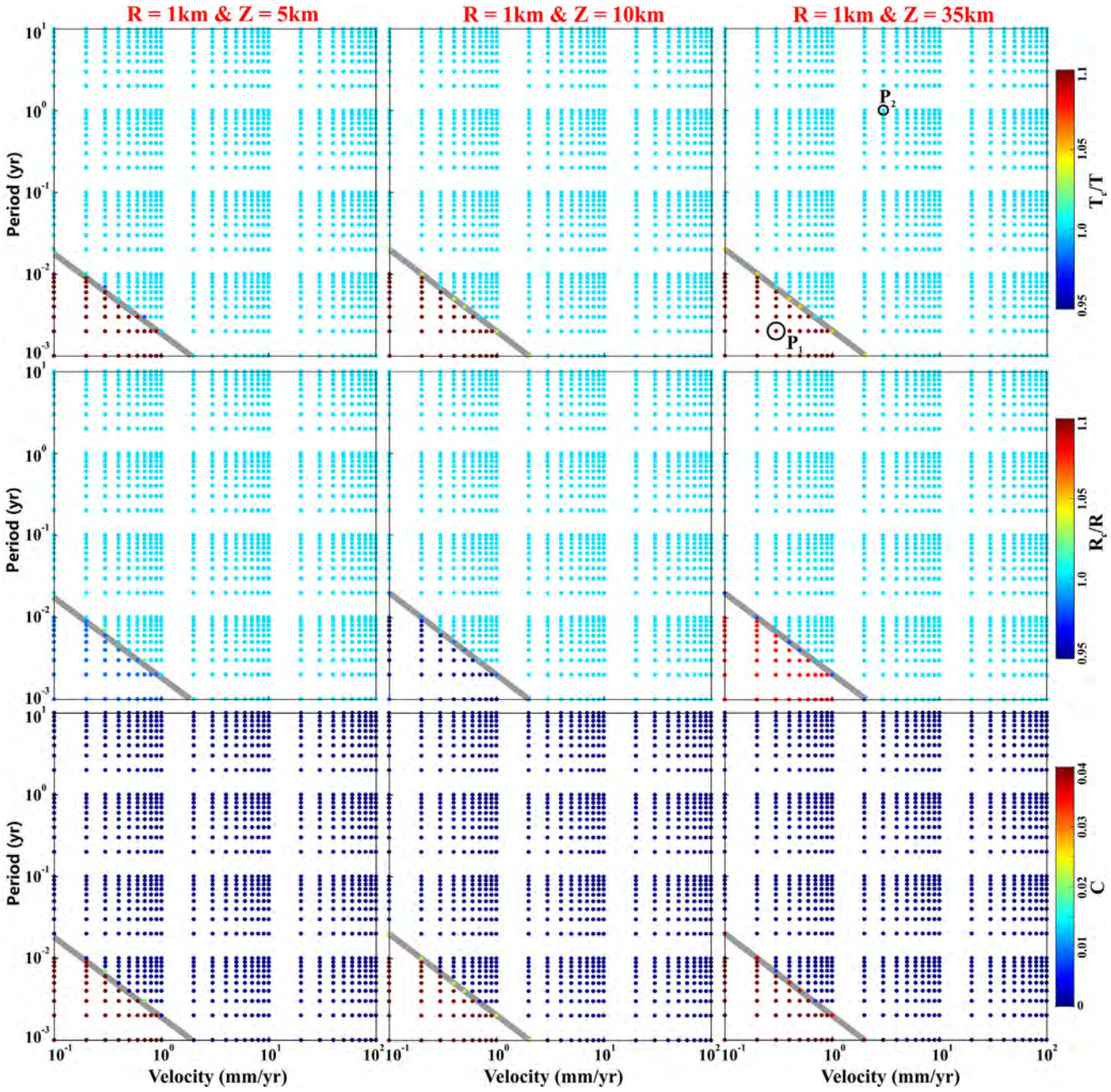

Fig. 2. Variation of the Fault resonance parameters that are estimated from the resonance destabilization process under rate-and-state dependent friction. The fault resonance parameters $\frac{T_c}{T}$, $\frac{R_c}{R}$ and cost function C are estimated from the resonance destabilization process by varying period of external stress perturbation (T) and velocity of the faults (V_L), assuming the length of the modulating fault patch or dimension of the slipping zone (R) as 1 km and depth of the seismicity (Z) as 5, 10 and 35 km respectively. The grey line demarcated the possible resonance destabilization zone to not possible resonance destabilization zone. It is clearly observed that short period modulation in the plate interior region is absent. Note that resonance destabilization occurred, when the critical period of external stress perturbation (T_c) is nearly equal to the period of external stress perturbation (T), The critical dimension of the slipping zone (R_c) is very close to the dimension of the slipping zone (R) and cost function C should be close to zero. A detailed explanation has been provided in the text (Section 4.1).

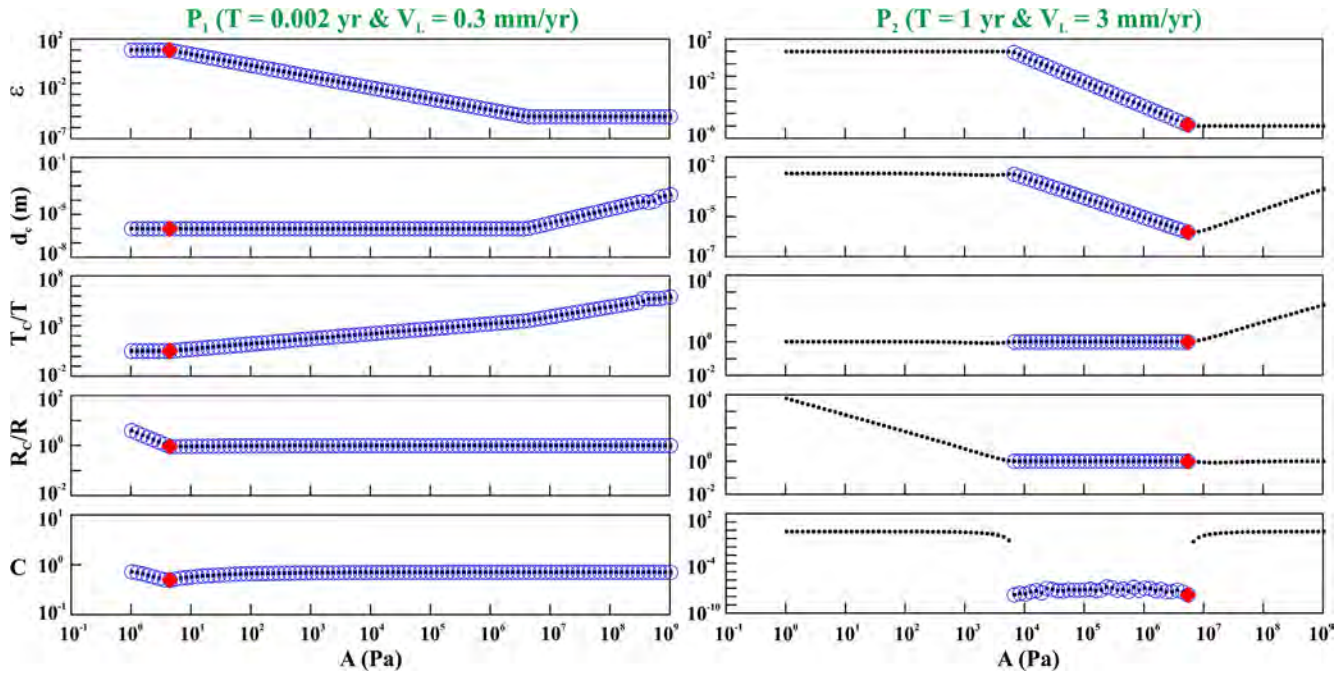

Fig. 3. Variations of the best-fit parameters of ε, d_c, $\frac{T_c}{T}$, $\frac{R_c}{R}$ and C as a function of the A parameter for a time period and velocity corresponding to P_1 and P_2 points, respectively (marked in Fig. 2). Where ε is the ratio of the frictional parameters a and b, d_c is the critical slip distance, R_c is the critical dimension of the slipping zone, R is the dimension of the slipping zone, T_c is the critical period of external stress perturbation, T is the period of external stress perturbation, and C is the cost function. The best-fit model corresponds to the red square and the blue circles define the range of acceptable models. Note that in the above two cases, the seismicity could be modulated by the resonance destabilization process for P_2 point in T vs. V_L spatial domain (T = 1 yr, V_L = 3 mm/yr), however, such modulation is lacking for P_1 point (T = 0.002 yr, V_L = 0.3 mm/yr). Note that resonance destabilization occurred, when the critical period of external stress perturbation (T_c) is nearly equal to the period of external stress perturbation (T), The critical dimension of the slipping zone (R_c) is very close to the dimension of the slipping zone (R) and cost function C should be close to zero.

stress perturbation factors that act on the brittle crust for seismicity modulation. Further, the length of the modulating fault patch or dimension of the slipping zone (R) varies from 1 km to 150 km in our simulation. In addition, the depth range of the seismicity modulation in the crust (Z) considers from surface to 35 km, as most of the seismogenic fault systems are associated with the crustal range.

Considering the above ranges of physical parameters in the resonance destabilization model, we have systematically tested the possibilities of the seismicity modulation process in V_L vs. T spatial domain (Figs. 2, 4, 6). To characterize the external stress perturbations induced resonance destabilization into our theoretical models, it must satisfy three criteria. The time-period of excitation (T) must be close to the critical period of excitation (T_c), the length of the fault patch (R) must be close to the critical length of fault patch (R_c), and finally, the cost function (C) should be close to zero. Therefore, resonance destabilization domains in the spatial plots are characterized by $\frac{T_c}{T} \rightarrow 1$, $\frac{R_c}{R} \rightarrow 1$, and $C \rightarrow 0$, and based on that, we have demarcated spatial domains in each V_L vs. T pots (i.e., marked by gray lines in Figs. 2, 4, 6). From this systematic analysis, it has been noted with an increasing dimension of the slipping zone (R) and depth range of the seismicity modulation in the crust (Z), the effective area of resonance destabilization domain gradually shrinks (i.e., decrease the area), with a gradual expansion of the non-resonance area in the each V_L vs. T spatial pots (Figs. 2, 4, 6). More explicitly, relatively short-period modulation (e.g., semidiurnal, diurnal and fortnight tidal constituents) appears to be impossible for stable plate interior (V_L = 0.01–2 mm/yr) and diffuse deformation boundary (V_L = 2–16 mm/yr), under resonance destabilization process. However, plate boundary region (V_L = 1 2–100 mm/yr) appears to be more susceptible for both short-period modulation (e.g., semi-diurnal and diurnal tidal constituents) and long-period modulation (e.g., fortnight tidal constituents; semi-annual, annual, pole tide, and pole wobble frequency). Further, we acknowledge that such characteristic feature remains stable, even if we consider a wide range of variation for R and Z.

In addition, Figs. 3, 5, 7 show the derived values ε, d_c, $\frac{T_c}{T}$, $\frac{R_c}{R}$, and C as a function of A for the hypothetical points (i.e., P_1 and P_2, marked in Figs. 2, 4, 6), assuming specific periods (T) and long-term plate motion velocity (V_L), respectively. The best-fit model parameter corresponds to the red square, and the range of admissible models, for which the cost function is reasonably small, are shown as blue circles (Figs. 3, 5, 7). All the figures show that only a limited range of A yields to low values of the cost function C. From this, it has been inferred that resonance destabilization and seismicity modulation can be possible for P_2 points. However, such modulation appears to be impossible for P_1 point in T vs. V_L spatial domains, based on the three criteria to satisfy the resonance destabilization process. We also suggest that laboratory values of rock friction experiments report a of 10^{-4} to 10^{-2} and d_c of 10^{-6} m to 10^{-2} m (Marone, 1998). Supplementary data Fig. S2 represents that for the resonance destabilization process of all presented theoretical models (Figs. 2, 4, 6), d_c has a narrow range of variations, ranging from 10^{-6} m to 10^{-3} m, which is further consistent with the laboratory estimates of this parameter (Marone, 1998).

4.2. Model validation with natural observations

To test the robustness of model prediction of resonant destabilization process, in this section, we have presented model validation, considering worldwide reports from diverse types of tectonic domains of seismicity modulation, stress perturbation by wide ranges of natural harmonic forcings. Fig. 8a represents the global distribution of reported seismicity modulation (including stable plate interior to plate boundaries) in response to various external stress perturbation and further projected over V_L vs. T spatial domain (Fig. 8b), considering specific time-periods (T) and

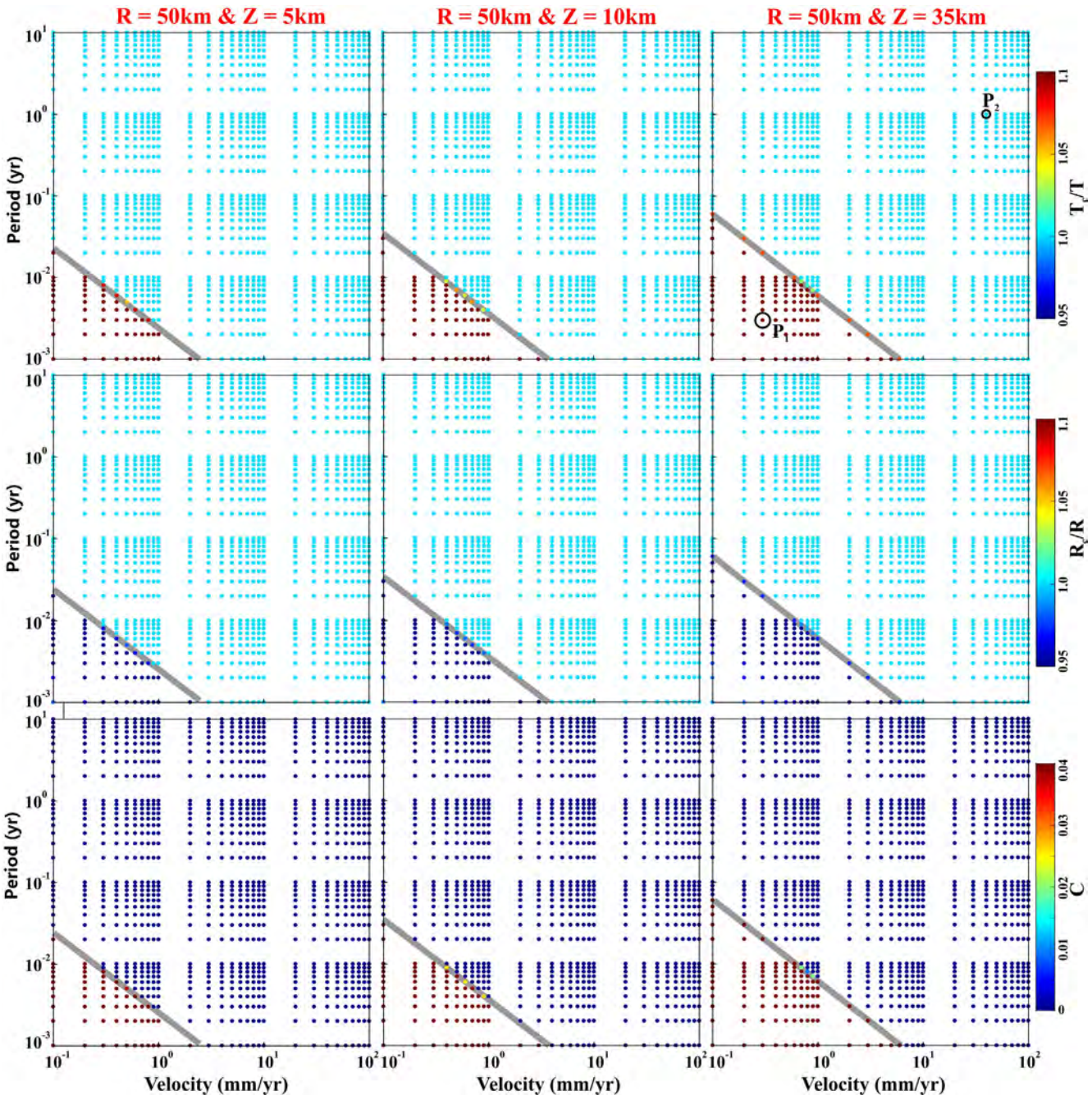

Fig. 4. Variation of the Fault resonance parameters that are estimated from the resonance destabilization process under rate-and-state dependent friction. The fault resonance parameters T_c/T, $\frac{R_c}{R}$, and cost function C are estimated from the resonance destabilization process by varying periods of external stress perturbation (T) and velocity of the faults (V_L), assuming the length of the modulating fault patch or dimension of the slipping zone (R) as 50 km and depth of the seismicity as 5, 10 and 35 km respectively. The grey line demarcated the possible resonance destabilization zone to not possible resonance destabilization zone. It is clearly observed that short period modulation in the plate interior region is absent. Note that resonance destabilization occurred, when the critical period of external stress perturbation (T_c) is nearly equal to the period of external stress perturbation (T), The critical dimension of the slipping zone (R_c) is very close to the dimension of the slipping zone (R) and cost function C should be close to zero. A detailed explanation has been provided in the text (Section 4.1).

long-term plate motion velocity (V_L) respectively. From these natural observations, it has been inferred that the relatively short-period modulation appears to be impossible for stable plate interior and diffuse deformation boundaries, whereas the long-period modulations appear to be more susceptible. However, the plate boundary regions (i.e., V_L > 10–12 mm/yr) are susceptible to both short-period and long-period modulation processes. This characteristic contrast in seismicity modulation appears to be a good agreement with the theoretical model prediction, which has been inferred from the resonance destabilization process.

Although this hypothesis can be challenged for shorter-periods (e.g., semi-diurnal, diurnal, fortnight, etc.) modulation, as most of the worldwide plate-boundary domains lie along the ocean-land boundary where stress on the interplate fault planes are more due to ocean-tidal loading than the solid-earth tide. On the other hand, only solid-earth tide works for intraplate faults, and this might make apparent insensitivity of intraplate earthquakes to short period tidal stress. However, in response to this argument, we have suggested the following explanation by considering different natural cases. From resonance destabilization model

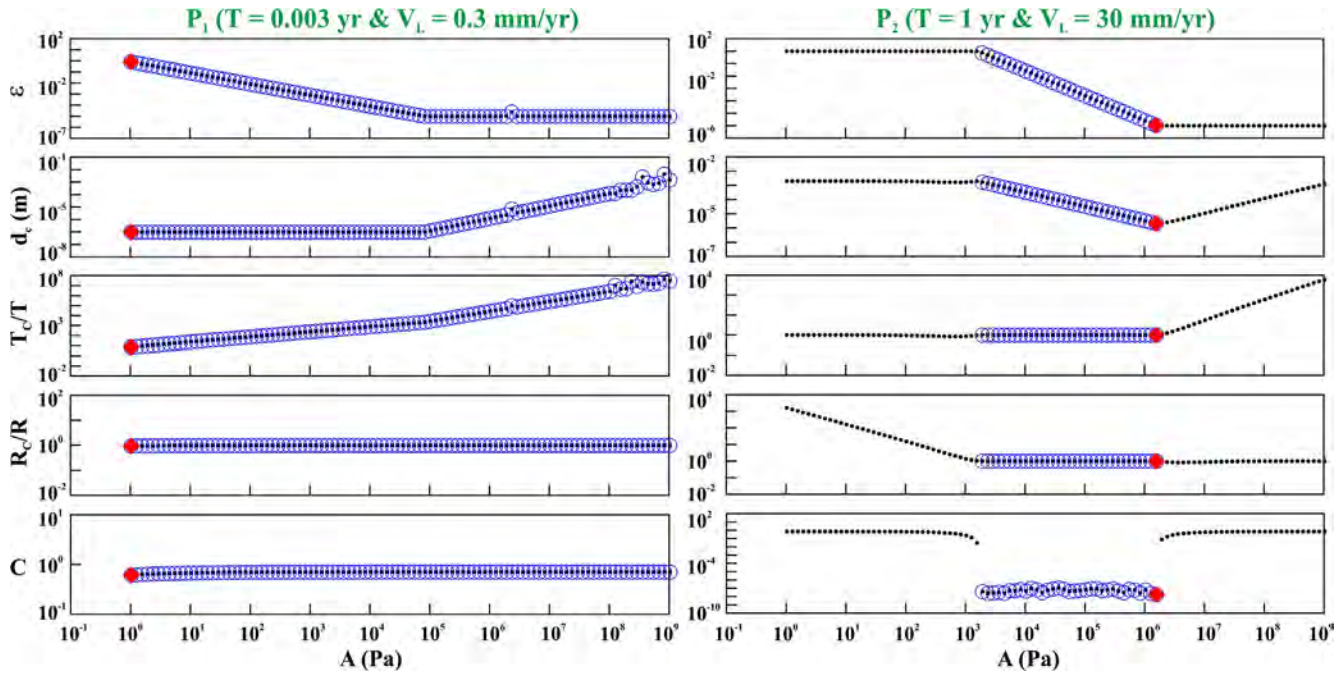

Fig. 5. Variations of the best-fit parameters of ε, d_c, $\frac{T_c}{T}$, $\frac{R_c}{R}$ and C as a function of the A parameter for a time period and velocity corresponding to P_1 and P_2 points, respectively (marked in Fig. 4). The best-fit model corresponds to the red square, and the blue circles define the range of acceptable models. Note that in the above two cases, the seismicity could be modulated by the resonance destabilization process for P_2 point in T vs. V_L spatial domain (T = 1 yr, V_L = 40 mm/yr), however, such modulation is lacking for P_1 point (T = 0.003 yr, V_L = 0.3 mm/yr).

(i.e., theoretically, under laboratory-based investigation and natural case study (Perfettini and Schmittbuhl, 2001; Perfettini et al., 2001; Boettcher and Marone, 2004; Lowry, 2006; Panda et al., 2018; Panda et al., 2020), it has been established that a very small insignificant amount external stress perturbation can destabilize the seismogenic fault systems and enter into a stick–slip domain. It has been reported that the annual hydrological load-induced stress is of the order of a few Pa to kPa and is well capable of modulating seismicity in low-strain stable plate interior (Craig et al., 2017) as well as in the plate boundary regions (Lowry, 2006; Panda et al., 2018). Therefore, we argue that amount or magnitude of purebred stress or its slight variation may not contribute much to this process.

Moreover, the well-established region like the Koyna-Warna seismic zone (Gupta, 2002), located on the western coast of stable peninsular India (Fig. 9a), can be considered as stable plate interior domains. Interestingly, it has been noted that the seismicity associated with Koyna-Warna seismic zone exhibits significant annual and semi-annual periodicity, and that has linked to the periodic reservoir water level fluctuation (Yadav et al., 2015), however short-period tidal periodicity (i.e., diurnal and semi-diurnal tidal constituents) is lacking (Fig. 9b,c). Although this stable plate interior region is located close to the coast in the open ocean, we should expect short-period tidal modulation of semi-diurnal (or diurnal) constituents as perturbed ocean-tidal loading stress is higher. However, such short-period tidal modulation is lacking in this region. We have also observed that the smaller magnitude level of seismicity (M 2–3) exhibits strong annual and semi-annual periodicity, whereas the seismicity of relatively larger magnitude (M > 3) does not show any such periodicity (Supplementary data Fig. S3). Further, in order to show the degree of correlation between the seismicity and reservoir load-induced stress perturbation, we have divided the seismicity catalogue magnitude wise and estimated the percentage of excess value (N_{ex}). The N_{ex} value is defined as the difference between the actual and total number of events divided by the total number of events (Cochran et al., 2004; Thomas et al., 2009):

$$N_{ex} = \frac{N_{exp} - \frac{1}{2}N_{total}}{N_{total}} \times 100 \quad (10)$$

where, N_{exp} is the number of events occurring during the encouraging loading period with phase (θ) of $90° \leq \theta \leq 270°$ (Cochran et al., 2004; Fig. 9e, Supplementary data Fig. S4) and N_{total} is the total number of events. From this analysis, we have observed that the smaller magnitude level of seismicity (M 2–3) exhibits a strong correlation with the reservoir load-induced stress perturbation (N_{ex} = 9%), however, the seismicity of relatively larger magnitude (M > 3) shows a very weak correlation with the stress (N_{ex} = –1.4%) (Fig. 9f, Supplementary data Fig. S5). Moreover, the New Madrid Seismic Zone in the central United States is probably one of the well-monitored seismically active plate-interior regions that have witnessed several significant earthquakes, including a devastating 1811–1812 earthquake sequence (Calais et al., 2010, 2016). The rate of micro-earthquakes in the New Madrid Seismic Zone has been correlated at annual and multi-annual timescales with periodic hydrological surface loading in the upper Mississippi embayment (Craig et al., 2017). However, it does not exhibit any short-period tidal modulation (i.e., semi-diurnal or diurnal constituents). In contrast, well-monitored non-volcanic tremor patches associated with the Cascadia subduction zone close to Vancouver Island (e.g. of classical plate boundary region), strongly modulated by both tidal loading (van der Elst et al., 2016) and annual hydrological loading (Pollitz et al., 2013). These observations are complemented with our theoretical model prediction under the resonance destabilization process (Fig. 8b, circular symbols 8, 1, 3 for Koyna-Warna seismic zone, New Madrid Seismic Zone, Cascadia, respectively).

Although the concept of tidal triggering was established more than a century (Schuster, 1897), even then, in many case studies of large samples of continental micro-seismicity, no significant correlation with tidal forcing has been reported (e.g., Heaton, 1982;

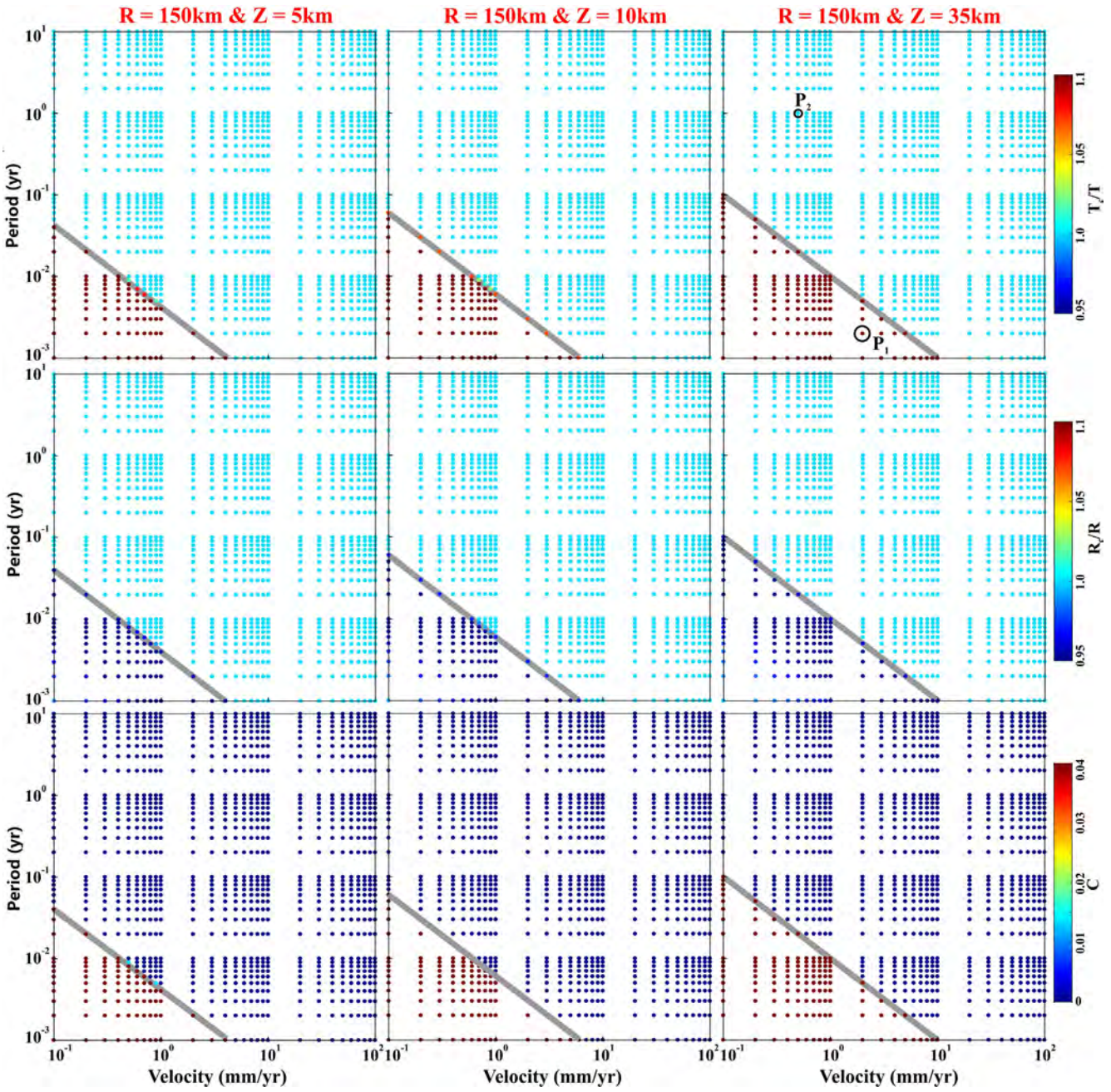

Fig. 6. Variation of the Fault resonance parameters that are estimated from the resonance destabilization process under rate-and-state dependent friction. The fault resonance parameters T_c/T, $\frac{R_c}{R}$, and cost function C are estimated from the resonance destabilization process by varying periods of external stress perturbation (T) and velocity of the faults (V_L), assuming the length of the modulating fault patch or dimension of the slipping zone (R) as 150 km and depth of the seismicity as 5, 10 and 35 km respectively. The grey line demarcated the possible resonance destabilization zone to not possible resonance destabilization zone. It is clearly observed that, short period modulation in the plate interior region is absent. Note that resonance destabilization occurred, when the critical period of external stress perturbation (T_c) is nearly equal to the period of external stress perturbation (T), The critical dimension of the slipping zone (R_c) is very close to the dimension of the slipping zone (R) and cost function C should be close to zero. A detailed explanation has been provided in the text (Section 4.1).

Vidale et al., 1998). Based on the analysis of a large global dataset of ~442,412 events, Métivier et al. (2009) argued for a significant tidal triggering signal that has enhanced for smaller magnitude and shallower earthquakes. In that context, we argued that network geometry and completeness of earthquake catalog with lower magnitude thresholds also play a significant role in detecting seismicity modulation. Investigations based on laboratory and rate-and-state friction study argue that tides and seismicity have strongly correlated if the nucleation duration of a seismic event is close to the period of the tidal forcing (Lockner and Beeler, 1999; Beeler and Lockner, 2003; Perfettini and Schmittbuhl, 2001; Ader et al., 2014). Based on laboratory studies, it has been further argued that the link between tidal stress amplitude and correlation with the earthquake triggering is relatively complex and a non-linear process (Rydelek et al., 1992; Lockner and Beeler, 1999; Beeler and Lockner, 2003).

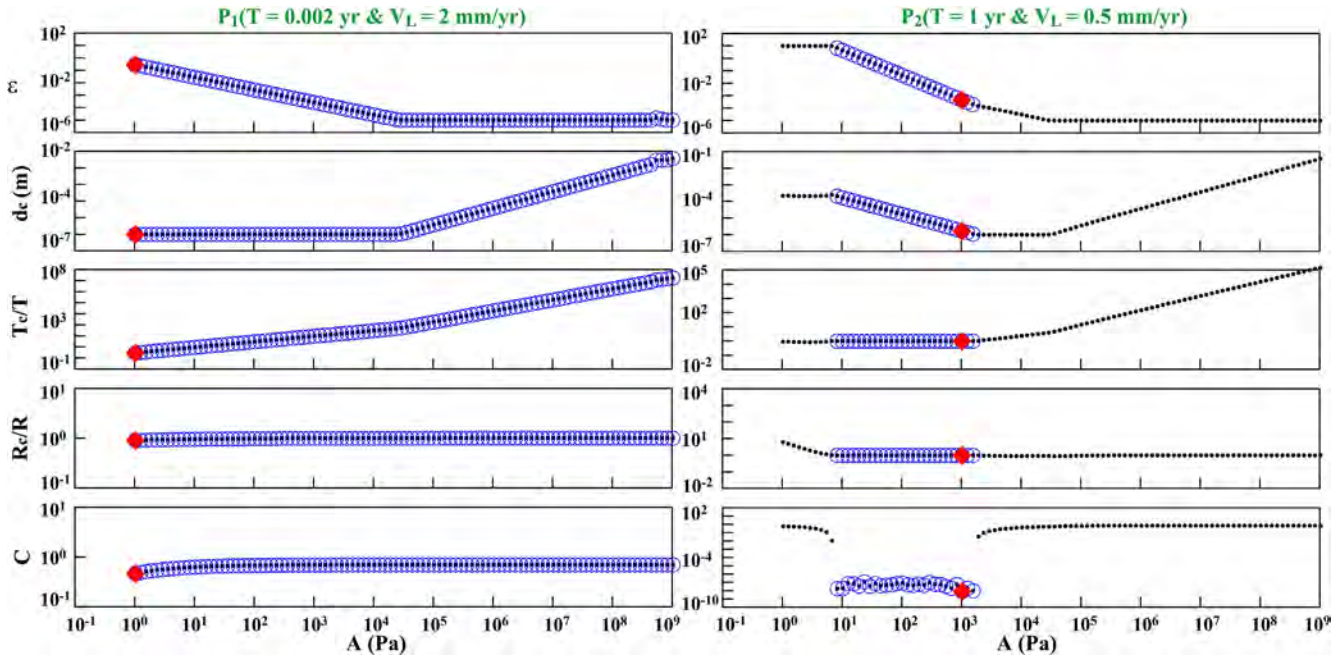

Fig. 7. Variations of the best-fit parameters of ε, d_c, $\frac{T_c}{T}$, $\frac{R_c}{R}$ and C as a function of the A parameter for a time period and velocity corresponding to P_1 and P_2 points, respectively (marked in Fig. 6). The best-fit model corresponds to the red square, and the blue circles define the range of acceptable models. Note that in the above two cases, the seismicity could be modulated by the resonance destabilization process for P_2 point in T vs. V_L spatial domain (T = 1 yr, V_L = 0.5 mm/yr), however, such modulation is lacking for P_1 point (T = 0.002 yr, V_L = 2 mm/yr).

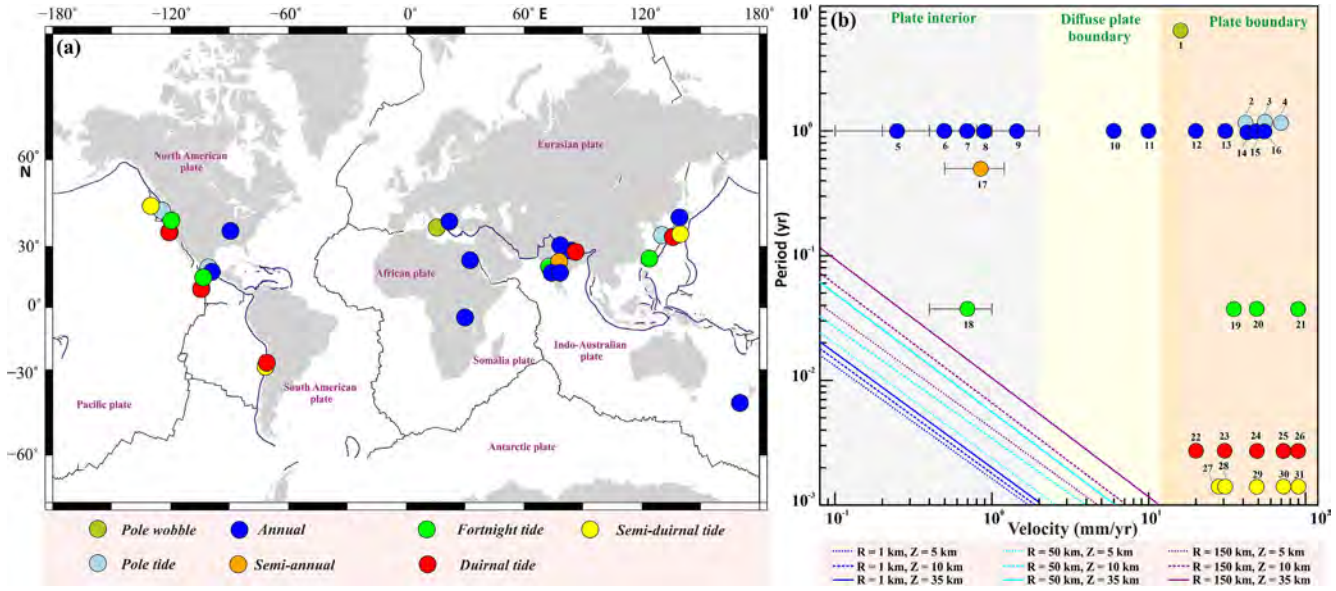

Fig. 8. Diversity in seismicity modulation observed in the worldwide plate boundary and plate interior domains. (a) Represents global distribution of seismicity modulation in a diverse type of tectonic setting and (b) comparison with theoretical model prediction related to resonance destabilization process. The different colour dots represent various observed seismicity modulation in worldwide. The different colour lines are obtain from the resonance destabilization model by varying periods (T), long-term velocity (V_L), assuming dimension of the slipping patch (R) 1, 50 and 150 km and depth of seismicity (Z) about 5, 10 and 35 km respectively. Note the overall absence of tidal modulation in the plate interior region. Nos. 1–27 represent various natural examples considered for complementing and validation for the resonance destabilization model. [1- (New Madrid Seismic zone), Craig et al., 2017; 2- (Mount Etna), Lambert and Sottili, 2019; 3, 4 5- (Cascadia, Mexico and Bungo channel), Shen et al., 2005; 6- (New Madrid Seismic zone), Craig et al., 2017; 7- (Aswan), Gahalaut et al., 2017; 8- (Koyan Warna seismic zone), Yadav et al., 2015; 9- (East Africa rift), Xue et al., 2020; 10- (Teheri), (Chander and Gahalaut, 1996; Gahalaut et al., 2017); 11- (Nepal), Kundu et al., 2017; 12- (Alpine fault), Oestreicher, 2018; 13- (San Andreas), Pollitz et al., 2013; Christiansen et al., 2007; 14- (Guerrero subduction zone), Lowry, 2006; 15- (Delhi), Tiwari et al., 2021; 16- (San Andreas), van der Elst et al., 2016; 17, 22 & 26- (East Pacific rise), Stroup et al., 2007; Tan et al., 2018; 18& 23- (Chile subduction zone), Gallego et al., 2013; 19 &24- (San Andreas), Thomas et al., 2009; 20 & 25- (Japan), (Rubinstein et al., 2008); 22- (Juan de Fuca ridge), Scholz et al., 2019; Sahoo et al., 2021].

5. Discussions

The strength of the seismogenic faults are mainly controlled by the combined effect of tectonic loading of diverse tectonic settings and various types of external loading process (e.g., hydrological load, tidal load, reservoir induced load. snow load, atmospheric load, etc.) (Johnson et al., 2017). Hence, it is important to understand the physics of the earthquake to predict the response

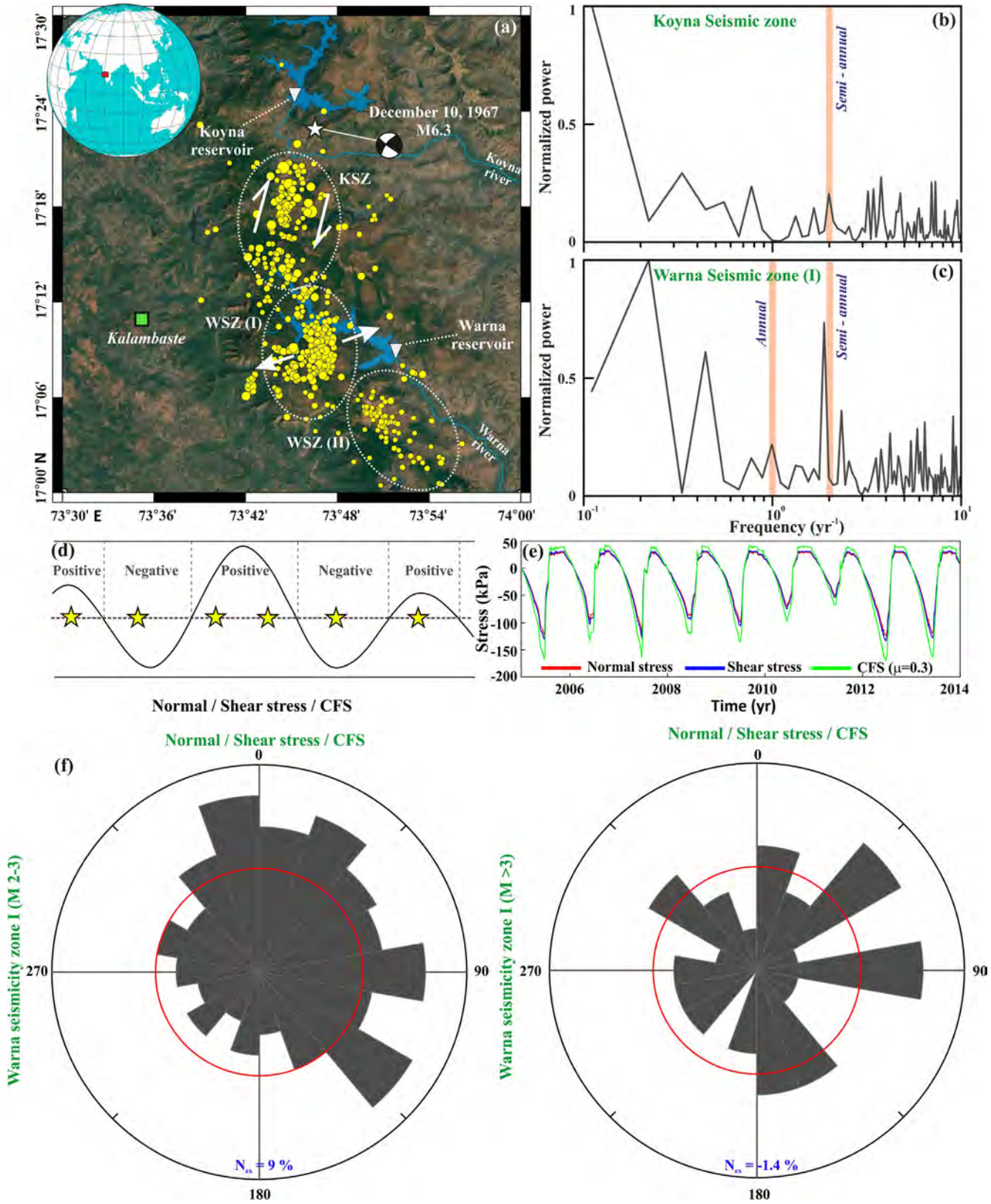

Fig. 9. (a) Spatial distribution of the declustered seismicity catalogue of Mc > 2.0 (shown by yellow circles) from the Koyna-Warna region for the time period of 2005–2013. White star indicates the location of the M6.3 earthquake along with its focal mechanism solution. The entire zone is divided into three segments based upon the spatial distribution of seismicity clusters, i.e., Koyna Seismic Zone (KSZ), Warna Seismic Zone (I), and Warna Seismic Zone (II). An inverted white triangle represents the location of the Koyna and Warna dam sites. The top inset shows the location of the Koyna-Warna region on the Indian sub-continent (taken from (Senapati et al., 2021)). (b, c) Power spectrum analysis of decluster seismicity catalogue (Mc > 2.0) from the Konya Seismic Zone (KSZ) and WSZ (I), respectively. Note that WSZ (I) shows annual and semi-annual periodicity, whereas KSZ shows semi-annual periodicity but no evidence of annual periodicity. Note that seismicity in WSZ II is mainly related to mining (anthropogenic) activity. Hence, we have not considered the WSZ II seismicity in our present study. (d) Schematic diagram showing the variation of reservoir induced normal/shear stress and the phase associated with it. The yellow star marks one hypothetical earthquake. (e) Reservoir induced normal, shear, and column failure stress (CFS) calculated from water level variation in the Konya–Warna reservoir. (f) Phase plot between the seismicity and reservoir induced normal shear and CFS. Note the seismicity (M 2–3) shows strong correlation with the reservoir-induced stress, whereas seismicity (M > 3) does not show any correlation with the reservoir-induced stress.

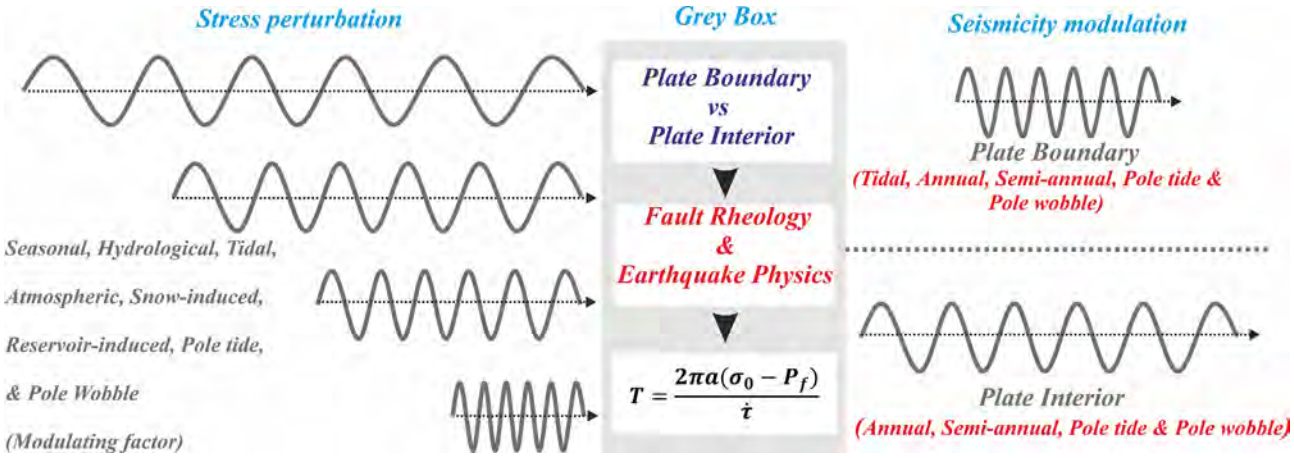

Fig. 10. Cartoon indicates the challenge in understanding seismicity modulation in response to exogenous modulating factors, considering fault interfaces governed by rate-and-state friction in earthquake physics. The earthquake physics, which predicts how a seismogenic faults system response to an imposed harmonic stress perturbation history, remains somewhat considered as a grey box. External stress perturbations of varying amplitudes and frequencies (left panel), can cause seismicity modulations that depend upon the critical time period (T). In the case of plate boundary and plate interior regions, the variation in secular loading rate ($\dot{\tau}$) and anomalous crustal fluid (P_f) significantly controls the variation and specific periods in seismicity modulations (short or longer periods). Note, In contrast, plater boundary region (i.e., sensitive for both long-period and short-period seismicity modulation), slowly deforming stable plate interior regions, and diffuse deformation zones appear to be more sensitive for long-period seismicity modulation in semi-annual, annual, or even multi-annual time scales, however less sensitive for short-period seismicity modulation.

of periodic stress perturbation on a seismogenic fault, which is like a grey box (Fig. 10). Further, the mechanisms that act on seismogenic fault has been well described by the rate-and-state friction (Dieterich, 1978, 1979; Ruina, 1983), where the seismicity modulations by the external stress perturbations depend upon the period of external stress perturbation (T) and secular loading rate (Ader et al., 2014). In the case of plate boundary regions, the variation in secular loading rate is very fast as compared to the plate interior domain. Therefore, both short-periods and long-period seismicity modulations are observed in the plate boundary regions (Fig. 10), whereas in the plate interior domain, only long-period seismicity modulation is observed (Fig. 10). Moreover, such periodic response of seismogenic faults has been observed in various laboratory experiments under variation of harmonic stress (Lockner and Beeler, 1999; Beeler and Lockner, 2003; Savage and Marone, 2007, 2008). They observed that when the periods of harmonic stress perturbations are larger than the critical period, the rate of stick–slip events (i.e., seismicity rate) are directly proportional to the rate of harmonic stress perturbation (Beeler and Lockner, 2003; Lockner and Beeler, 1999).

Further, the threshold value of the external stress perturbations is also very important to understand the modulation of the seismicity. It has observed the critical threshold for stress perturbation value about 0.15–0.3 kPa for tides (Thomas et al., 2009), less than 2 kPa for rainfall-induced earthquakes (Hainzl et al., 2006), 0.05–0.15 kPa/yr for groundwater unloading induced triggering of 2015 Gorkha Earthquake in Nepal (Kundu et al., 2015), 0.1–10 kPa for seismic waves (Peng et al., 2009; Gomberg, 2010), 0.1–1 kPa for hydrological load-induced non-volcanic tremor along the Cascadia subduction zone (Pollitz et al., 2013). However, Ziv and Rubin (2000) have studied the lower threshold value of external stress perturbation for the earthquake triggering process and suggested that, there is no lower threshold exists for earthquake triggering in central California. Hence, we suggested that a very small variation of the external stress perturbation may be capable to destabilized the fault system and entering into the stick–slip regime by fault resonance process, as well as modulating the seismicity.

We argue that the tidal induced stress amplitude in plate boundary regions is much larger than the plate interior region due to large ocean tidal loading effect, as most of the plate-boundary regions are located near to the coastal region. For example, the Koyna-Warna seismic zone, which is a well know stable plate interior region and located near to the western coast of India (Fig. 9a). Therefore, we should expect short-period tidal modulation (i.e., semi-diurnal, diurnal, fortnight, etc.), since ocean-tidal loading stress perturbation is significantly larger in this coastal region. However, such short-period tidal modulation is absent in this plate interiopr region (Supplementary data Fig. S3, Fig. 9b,c). In contrast, the seismicity associated with Koyna-Warna seismic zone exhibits statistically significant annual and semi-annual periodicity (Fig. 9b, d), which is linked to the periodic reservoir water level fluctuation. Therefore, we suggest that the lack of case study to support their presence should not be considered as evidence for their absence.

We also argue that, with a slight variation of fault frictional parameters, phase-lag between the responses of the critically stressed faults system and exogenous stress perturbations close to resonance represents uncorrelated scattering (Perfettini and Schmittbuhl, 2001), and hence we do not expect seismicity modulation in that case (Supplementary data Fig. S6). Moreover, we cannot rule out other complex fault-rheological processes, which also have influenced the seismicity modulation process along seismogenic faults. In fact, the post-seismic recovery of locking (Yuzariyadi and Heki, 2021), the time required for fault gauge accumulation, time-dependent fault frictional property (Scholz, 1988; Scholz, 1998), the migration of fluids (Kodaira et al., 2004), and anomalous fluid pressure associated with the seismogenic fault systems (Dunn et al., 2013; Bisrat et al., 2012; Patro et al., 2017) cannot be neglected.

6. Conclusions

From this comprehensive study based on resonance destabilization model under rate-and-state dependent frictional formalism and comparison with globally documented seismicity modulation in wide ranges of tectonic settings (i.e., stable plate interior to relatively faster-moving plate boundary domains), the following key conclusions are found:

(i) Stable plate interior regions and diffuse deformation zones appear to be more sensitive for long-period seismicity modulation in response to naturally reported harmonic forcing, while short-period seismicity modulation appears to be less sensitive in the view of the resonance destabilization model. However, in contrast relatively faster-moving plate boundary regions are equally susceptible for both short-period and long-period seismicity modulation processes in response to stress perturbation from natural harmonic forcing.

(ii) The magnitude of external stress perturbation or its variation does not contribute much to the resonance destabilization and subsequent seismicity modulation process. Rather we argued that a very small insignificant amount of external stress perturbation (i.e., few Pa to kPa order) even could destabilize the seismogenic fault systems.

(iii) The seismicity modulation in diverse types of active tectonic settings behaves like a gray box analogy, and the presence of anomalous crustal fluid, variation in frictional parameters, background stress level, specific fault rheology, fault gauge accumulation, etc. can also make the seismic triggering/-modulation process relatively complex and non-linear. The mechanism of seismicity modulation deserves much scientific attention in the near future.

Declaration of Competing Interest

The authors declare that they have no known competing financial interests or personal relationships that could have appeared to influence the work reported in this paper.

Acknowledgement

This work has been performed within the framework of Batakrushna Senapati's Ph.D. thesis at NIT Rourkela. We thank N. Purnachandra Rao for sharing the seismicity catalog of the Koyna-Warna seismic zone. We thank Hugo Perfettini for technical guidance in developing modeling code for the resonance destabilization process. We also thank K. Heki for their constructive comments and suggestions, which significantly improved the results and presentation in the draft. BS has been supported by the NITR research fellowship. This work is financially supported by the Ministry of Earth Sciences (Seismology Division), Govt. of India, through grant number (MoES/P.O(Seismo)/1(349)/2018) to Bhaskar Kundu. All the other relevant information and modeling code for resonance destabilization are available from the corresponding author upon reasonable request. All the other information used in the present work is available openly in the public domain and presented in the text and supporting documents. We thank the Associate Editor Dr. C.J. Spencer and two anonymous reviewers for their constructive comments and suggestions, which significantly improved the quality of the work.

Appendix A. Supplementary data

Supplementary data to this article can be found online at https://doi.org/10.1016/j.gsf.2022.101352.

References

Ader, T.J., Lapusta, N., Avouac, J.-P., Ampuero, J.-P., 2014. Response of rate-and-state seismogenic faults to harmonic shear-stress perturbations. Geophys. J. Int. 198 (1), 385–413.

Arvidsson, R., 1996. Fennoscandian earthquakes: whole crustal rupturing related to postglacial rebound. Science 274 (5288), 744–746.

Beeler, N.M., Lockner, D.A., 2003. Why earthquakes correlate weakly with the solid Earth tides: Effects of periodic stress on the rate and probability of earthquake occurrence. J. Geophys. Res. 108 (B8), 2391.

Bettinelli, P., Avouac, J.-P., Flouzat, M., Bollinger, L., Ramillien, G., Rajaure, S., Sapkota, S., 2008. Seasonal variations of seismicity and geodetic strain in the Himalaya induced by surface hydrology, Earth planet. Sci. Lett. 266 (3-4), 332–344.

Bilham, R., Bendick, R., Wallace, K., 2003. Flexure of the Indian plate and intraplate earthquakes. J. Earth Syst. Sci. 112 (3), 315–329.

Bisrat, S.T., DeShon, H.R., Rowe, C.A., 2012. Swarm activity within the New Madrid seismic zone identified using waveform cross correlation techniques. Bull. Seismol. Soc. Am. 102, 1167–1178.

Boettcher, M.S., Marone, C., 2004. Effects of normal stress variation on the strength and stability of creeping faults. J. Geophys. Res. 109, B03406.

Bollinger, L., Perrier, F., Avouac, J.-P., Sapkota, S., Gautam, U., Tiwari, D.R., 2007. Seasonal modulation of seismicity in the Himalaya of Nepal. Geophys. Res. Lett. 34 (8).

Calais, E., Camelbeeck, T., Stein, S., Liu, M., Craig, T.J., 2016. A new paradigm for large earthquakes in stable continental plate interiors. Geophys. Res. Lett. 43, 10621–10637.

Calais, E., Freed, A.M., Van Arsdale, R., Stein, S., 2010. Triggering of New Madrid seismicity by late-Pleistocene erosion. Nature. 466 (7306), 608–611.

Campbell, D.L., 1978. Investigation of the stress concentration mechanism for intraplate earthquakes. Geophys. Res. Lett. 5 (6), 477–479.

Chanard, K., Avouac, J.P., Ramillien, G., Genrich, J., 2014. Modeling deformation induced by seasional variations of continental water in the Himalaya region: Sensitivity of Earth elastic structure. J. Geophys. Res. Solid Earth. 119, 5097–5113.

Chander, A., Gahalaut, K., 1996. Probable influence of Tehri reservoir on earthquakes of Garhwal Himalaya. Current science. 70, 4.

Christiansen, L.B., Hurwitz, S., Ingebritsen, S.E., 2007. Annual modulation of seismicity along the San Andreas Fault near Parkfield. CA. Geophys. Res. Lett. 34, L04306.

Cochran, E.S., Vidale, J.E., Tanaka, S., 2004. Earth tides can trigger shallow thrust fault earthquakes. Science 306 (5699), 1164–1166.

Cooper, C.M., Miller, M.S., Moresi, L., 2017. The structural evolution of the deep continental lithosphere. Tectonophysics 695, 100–121.

Costain, J.K., Bollinger, G.A., Speer, J.A., 1987. Hydroseismicity—A hypothesis for the role of water in the generation of intraplate seismicity. Geology 15 (7), 618–621.

Craig, J.T., Chanard, K., Calais, E., 2017. Hydrologically-driven crustal stresses and seismicity in the New Madrid Seismic Zone. Nat. Commun. 8, 2143.

Crone, A.J., De Martini, P.M., Machette, M.N., Okumura, K., Prescott, J.R., 2003. Paleoseismicity of two historically quiescent faults in Australia: Implications for fault behavior in stable continental regions. Bull. Seismol. Soc. Am. 93 (5), 1913–1934.

Dieterich, J.H., 1978. Time-dependent friction and the mechanics of stickslip. Pure appl. Geophys. 116, 790–806.

Dieterich, J.H., 1979. Modeling of rock friction 2: simulation of preseismic slip. J. Geophys. Res. 84 (B5), 2169.

Dunn, M., DeShon, H.R., Powell, C.A., 2013. Imaging the New Madrid Seismic Zone using double-difference tomography. J. Geophys. Res. Solid Earth. 118 (10), 5404–5416.

Eshelby, J., 1957. The determination of the elastic field of an ellipsoidal inclusion and related problems. Proc. Roy. Soc. London Series A 241, 376–396.

Foster, J.H., Lowry, A.R., Brooks, B.A., 2013. Fault frictional parameters and material properties revealed by slow slip events at Kilauea volcano. Hawaii. Geophys. Res. Lett. 40 (23), 6059–6063.

Foulger, G.R., Wilson, M.P., Gluyas, J.G., Julian, B.R., Davies, R.J., 2018. Global review of human-induced earthquakes. Earth-Sci. Rev. 178, 438–514.

Fu, Y., Freymueller, J.T., 2012. Seasonal and long-term vertical deformation in the Nepal Himalaya constrained by GPS and GRACE measurements. J. Geophys. Res. 117, B03407.

Fu, Y., Freymueller, J.T., Jensen, T., 2012. Seasonal hydrological loading in southern Alaska observed by GPS and GRACE. Geophys. Res. Lett. 39, L15310.

Gahalaut, K., Hassoup, A., Hamed, H., Kundu, B., Gahalaut, V., 2017. Long-Term and Annual Influence of Aswan Reservoir (Egypt) on the Local Seismicity: A Spatio-Temporal Statistical Analysis. Pure Appl. Geophys. 174 (1), 133–150.

Gahalaut, V.K., Yadav, R.K., Sreejith, K.M., Kalpna, G., B¨urgmann, R., Agrawal, A., Sati, S.P., Bansal, A., 2017. InSAR and GPS measurements of crustal deformation due to seasonal loading of Tehri reservoir in Garhwal Himalaya. India. Geophys. J. Int. 209, 425–433.

Gallego, A., Russo, R.M., Comte, D., Mocanu, V., Murdie, R.E., VanDecar, J.C., 2013. Tidal modulation of continuous nonvolcanic seismic tremor in the Chile triple junction region. Geochem. Geophys. Geosyst. 14 (4), 851–863.

Gomberg, J., 2010. Lessons from (triggered) tremor. J. Geophys. Res. 115, B10302.

González, P.J., Tiampo, K.F., Palano, M., Cannavó, F., Fernández, J., 2012. The 2011 Lorca earthquake slip distribution controlled by groundwater crustal unloading. Nature Geosci. 5 (11), 821–825.

Gordon, R.G., 1998. The plate tectonic approximation: plate nonrigidity, diffuse plate boundaries, and global plate reconstructions. Ann. Rev. Earth planet. Sci., 26, 615–642.

Gross, S., Burgmann, R., 1998. Rate and state of background stress estimated from the aftershocks of the 1989 Loma Prieta, California, earthquake. J. Geophys. Res. 103 (B3), 4915–4927.
Gross, S., Kisslinger, C., 1997. Estimating tectonic stress rate and state with Landers aftershocks. J. Geophys. Res. 102 (B4), 7603–7612.
Gupta, H.K., 2002. A review of recent studies of triggered earthquakes by artificial water reservoirs with special emphasis on earthquakes in Koyna. India. Earth-Sci. Rev. 58 (3-4), 279–310.
Hainzl, S., Kraft, T., Wassermann, J., Igel, H., Schmedes, E., 2006. Evidence for rainfall-triggered earthquake activity. Geophys. Res. Lett. 33, L193003.
Hampel, A., Hetzel, R., Densmore, A.L., 2007. Postglacial slip rate increase on the Teton normal fault, northern Basin and Range Province, caused by melting of the Yellowstone ice cap and deglaciation of the Teton Range? Geology 35 (12), 1107.
Heaton, T.H., 1982. Tidal triggering of earthquakes. Bull. Seismol. Soc. Am. 72 (6), 2181–2200.
Heki, K., 2003. Snow load and seasonal variation of earthquake occurrence in Japan, Earth Planet. Sci. Lett. 207 (1-4), 159–164.
Johnson, C.W., Fu, Y., Bürgmann, R., 2017. Stress models of the annual hydrospheric, atmospheric, thermal, and tidal loading cycles on California faults: Perturbation of background stress and changes in seismicity. J. Geophys. Res.-Solid. Earth 122, 10605–10625.
Johnson, K.M., Shelly, D.R., Bradley, A.M., 2013. Simulations of tremor-related creep reveal a weak crustal root of the San Andreas Fault. Geophys. Res. Lett. 40 (7), 1300–1305.
Johnston, P., Wu, P., Lambeck, K., 1998. Dependence of horizontal stress magnitude on load dimension in glacial rebound models. Geophys. J. Int. 132 (1), 41–60.
Kaniuth, K., Vetter, S., 2006. Estimating atmospheric pressure loading regression coefficients from GPS observations. GPS Solut. 10 (2), 126–134.
Katsube, A., Kondo, H., Taniguchi, K., Kase, Y., 2017. Surface rupture and slip associated with the 2014 Nagano-ken Hokubu earthquake (Mw6.2). J. Geol. Soc. Jpn. 123 (1), 1–21.
Kodaira, S., Iidaka, T., Kato, A., Park, J.-O., Iwasaki, T., Kaneda, Y., 2004. High Pore Fluid Pressure May Cause Silent Slip in the Nankai Trough. Science 304 (5675), 1295–1298.
Kondo, H., Owen, L.A., 2013. Paleoseismology. In: Shroder, J.F. (Ed.), Treatise on Geomorphology. Academic Press, Cambridge, pp. 267–299.
Kundu, B., Vissa, N.K., Gahalaut, K., Gahalaut, V.K., Panda, D., Malik, K., 2019. Influence of anthropogenic groundwater pumping on the 2017 November 12 M 7.3 Iran-Iraq border earthquake. Geophys. J. Int. 218 (2), 833–839.
Kundu, B., Vissa, N.K., Gahalaut, V.K., 2015. Influence of anthropogenic groundwater unloading in Indo-Gangetic plains on the 25 April 2015 Mw 7.8 Gorkha. Nepal earthquake. Geophys. Res. Lett. 42 (24), 10,607–10,613.
Kundu, B., Vissa, N.K., Panda, D., Jha, B., Asaithambi, R., Tyagi, B., Mukherjee, S., 2017. Influence of a meteorological cycle in mid-crustal seismicity of the Nepal Himalaya. J. Asian Earth Sci. 146, 317–325.
Lambert, S., Sottili, G., 2019. Is there an influence of the pole tide on volcanism? Insights from Mount Etna recent activity. Geophys. Res. Lett. 46 (23), 13730–13736.
Landgraf, A., Kübler, S., Hintersberger, E., Stein, S., 2016. Active tectonics, earthquakes and palaeoseismicity in slowly deforming continents. Geological Society London, Special Publications 432 (1), 1–12. https://doi.org/10.1144/SP432.13.
Liu, ChiChing, Linde, A.T., Sacks, I.S., 2009. Slow earthquakes triggered by typhoons. Nature 459 (7248), 833–836.
Lockner, D.A., Beeler, N.M., 1999. Premonitory slip and tidal triggering of earthquakes. J. Geophys. Res.-Solid. Earth 104 (B9), 20133–20151.
Lowry, A.R., 2006. Resonant slow fault slip in subduction zones forced by climatic load stress. Nature 442 (7104), 802–805.
Luttrell, K., Sandwell, D., 2010. Ocean loading effects on stress at near shore plate boundary fault systems. J. Geophys. Res. 115, B08411.
Mahesh, P., Catherine, J.K., Gahalaut, V.K., Kundu, B., Ambikapathy, A., Bansal, A., Premkishore, L., Narsaiah, M., Ghavri, S., Chadha, R.K., Choudhary, P., Singh, D.K., Singh, S.K., Kumar, S., Nagarajan, B., Bhatt, B.C., Tiwari, R.P., Kumar, A., Kumar, A., Bhu, H., Kalita, S., 2012a. Rigid Indian plate: constraints from GPS measurements. Gondwana Res. 22 (3-4), 1068–1072.
Mahesh, P., Gahalaut, V.K., Catherine, J.K., Ambikapathy, A., Kundu, B., Bansal, A., Chadha, R.K., Narsaiah, M., 2012b. Localized crustal deformation in the Godavari failed rift. India. Earth Planet. Sci. Lett. 333-334, 46–51.
Marone, C., 1998. Laboratory-derived friction laws and their application to seismic faulting. Annu. Rev. Eath Planet. Sci. 26 (1), 643–696.
Mazzotti, S., 2007. Geodynamic models for earthquake studies in intraplate North America, in Continental Intraplate Earthquakes: Science, Hazard, and Policy Issues. , Geol.Soc. Am. Spec. Pap., 425, 17–33.
McGarr, A., Simpson, D., Seeber, L., 2002. Case histories of induced and triggered seismicity. In: Lee, W.H., Jennings, P., Kisslinger, C., Kanamori, H. (Eds.), International Geophysics Series, International Handbook of Earthquake and Engineering Seismology. pp. 647-664.
Métivier, L., de Viron, O., Conrad, C.P., Renault, S., Diament, M., Patau, G., 2009. Evidence of earthquake triggering by the solid Earth tides. Earth Planet Sci Lett. 278 (3-4), 370–375.
Obara, K., Kato, A., 2016. Connecting slow earthquakes to huge earthquakes. Science 353 (6296), 253–257.
Oestreicher, N.K., 2018. Geodetic, hydrologic and seismological signals associated with precipitation and in Itration in the central Southern Alps, New Zealand. Victoria University of Wellington. M.S thesis.
Okumura, K., 2001. Paleoseismology of the Itoigawa-Shizuoka tectonic line in central Japan. J. Seismolog. 5, 411–431.
Pal, D., Kundu, B., Santosh, M., 2018. Topography as a proxy for inter-plate coupling. J. Geodyn. 121, 133–142.
Panda, D., Kundu, B., Gahalaut, V.K., Bürgmann, R., Jha, B., Asaithambi, R., Yadav, R. K., Vissa, N.K., Bansal, A.K., 2018. Seasonal modulation of deep slow-slip and earthquakes on the Main Himalayan Thrust. Nat. Commun. 9 (1), 4140.
Panda, D., Kundu, B., Gahalaut, V.K., Bürgmann, R., Jha, B., Asaithambi, R., Yadav, R. K., Vissa, N.K., Bansal, A.K., 2020. Reply to "A warning against over-interpretation of seasonal signals measured by the Global Navigation Satellite System. Nat. Commun. 11 (1), 1–2.
Panda, D., Mondal, A., Kundu, B., 2019. Eastward "glacier-like flow" of the Tibetan crust constrained from power-law rheology. J. Asian Earth Sci. 177, 129–133.
Patro, P.K., Borah, U.K., Ashok Babu, G., Veeraiah, B., Sarma, S.V.S., 2017. Ground Electrical and Electromagnetic Studies in Koyna-Warna Region. India. J Geol Soc India. 90 (6), 711–719.
Peng, Z., Vidale, J.E., Wech, A.G., Nadeau, R.M., Creager, K.C., 2009. Remote triggering of tremor along the San Andreas Fault in central California. J. Geophys. Res. 114, B00A06.
Perfettini, H., Schmittbuhl, J., 2001. Periodic loading on a creeping fault: Implications for tides. Geophys. Res. Lett. 28 (3), 435–438.
H. Perfettini Frottement sur une faille: influence des fluctuations de la contrainte normale. Ph.D. Thesis, Université Pierre et Marie Curie (in French with English abstract) 2000
Perfettini, H., Molinari, A., 2017. A micromechanical model of rate and state friction:1. static and dynamic sliding. J. Geophys. Res. 122, 2590–2637. https://doi.org/10.1002/2016JB013, 302.
Perfettini, H., Schmittbuhl, J., Rice, J.R., Cocco, M., 2001. Frictional response induced by time-dependent fluctuations of the normal loading. J. Geophys. Res. 106 (B7), 13455–13472.
Pollitz, F.F., Kellogg, L., Bürgmann, R., 2001. Sinking mafic body in a reactivated lower crust: A mechanism for stress concentration at the New Madrid seismic zone. Bull. Seismol. Soc. Am. 91, 1882–1897.
Pollitz, F.F., Wech, A., Kao, H., Bürgmann, R., 2013. Annual modulation of non-volcanic tremor in northern Cascadia. J. Geophys. Res. Solid Earth 118 (5), 2445–2459.
Ramkumar, M.u., Menier, D., Mathew, M., Santosh, M., 2016. Geological, geophysical, and inherited tectonic imprints on the climate and contrasting coastal geomorphology of the Indian peninsula. Gondwana Res. 36, 65–93.
Ramkumar, M., Menier, D., Mathew, M., Santosh, M., Siddiqui, N.A., 2017. Early Cenozoic rapid flight enigma of the Indian subcontinent resolved: Roles of topographic top loading and subcrustal erosion. Geosci. Front. 8 (1), 15–23.
Rice, J.R., 1993. Spatio-temporal complexity of slip on a fault. J. Geophys. Res. 98 (B6), 9885. https://doi.org/10.1029/93JB00191.
Royer, J.Y., Gordon, R.G., 1997. The motion and boundary between the Capricorn and Australian plates. Science 277 (5330), 1268–1274.
Rubinstein, J.L., Mario La Rocca, M.L., John E. Vidale, J.E., Creager, K.C., Wech, A.G., et al., 2008. Tidal Modulation of Nonvolcanic Tremor. Science 319, 186. https://doi.org/10.1126/science.1150558.
Ruina, A., 1983. Slip instability and state variable friction laws. J. Geophys. Res. 88 (B12), 10359–10370.
Rydelek, P.A., Sacks, I.S., Scarpa, R., 1992. On tidal triggering of earthquakes at Camp Flegrei, Italy. Geophys. J. Int. 109, 125–1376.
Sahoo, S., Senapati, B., Panda, D., Tiwari, D.K., Santosh, M., Kundu, B., 2021. Tidal triggering of micro-seismicity associated with caldera dynamics in the Juan de Fuca ridge. J. Volcanol. Geotherm. Res. 417, 107319. https://doi.org/10.1016/j.jvolgeores.2021.107319.
Sauber, J., Plafker, G., Molnia, B.F., Bryant, M.A., 2000. Crustal deformation associated with glacial fluctuations in the eastern Chugach Mountains Alaska. J. geophys. Res. 105 (B4), 8055–8077.
Savage, H.M., Marone, C., 2007. Effects of shear velocity oscillations on stick-slip behavior in laboratory experiments. J. Geophys. Res. 112, B02301.
Savage, H.M., Marone, C., 2008. Potential for earthquake triggering from transient deformations. J. Geophys. Res. 113, B05302.
Scholz, C.H., Aviles, C.A., Wesnousky, S.G., 1986. Scaling differences between large interplate and intraplate earthquakes. Bull. Seismol. Soc. Am. 76 (1), 65–70.
Scholz, C.H., Tan, Y.J., Albino, F., 2019. The mechanism of tidal triggering of earthquakes at mid-ocean ridges. Nat. Commun. 10 (1), 2526.
Scholz, C.H., 1988. The critical slip distance for seismic faulting. Nature 336 (6201), 761–763.
Scholz, C.H., 1998. Earthquakes and friction laws. Nature 391 (6662), 37–42.
Schultz, R., Skoumal, R.J., Brudzinski, M.R., Eaton, D., Baptie, B., Ellsworth, W., 2020. Hydraulic fracturing-induced seismicity. Reviews of Geophysics 58. https://doi.org/10.1029/2019RG000695.
Schuster, A., 1897. On lunar and solar periodicities of earthquakes. Proc. R. Soc. Lond. 61, 455–465.
Schweig, E.S., Ellis, M.A., 1994. Reconciling short recurrence intervals with minor deformation in the New Madrid seismic zone. Science 264 (5163), 1308–1311.
Senapati, B., Kundu, B., Perfettini, H., Gahalaut, V.K., Singh, A.K., Ghosh, A., Rao, P., 2021. Fault resonance process and its implications on seismicity modulation on active Fault system. Geophys. J. Int. Submitted for publication.
Shen, Z.-K., Wang, Q., Burgmann, R., Wan, Y., Ning, J., 2005. Pole-Tide Modulation of Slow Slip Events at Circum-Pacific Subduction Zones. Bull. Seismol. Soc. Am. 95 (5), 2009–2015.
Sieh, K.E., 1984. Lateral offsets and revised dates of large prehistoric earthquakes at Pallett Creek, southern California. J. Geophys. Res. 89 (B9), 7641–7670.

Stein, S., Liu, M., 2009. Long aftershock sequences within continents and implications for earthquake hazard assessment. Nature 462 (7269), 87–89.
Stewart, I.S., Sauber, J., Rose, J., 2000. Glacio-seismotectonics: ice sheets, crustal deformation and seismicity. Quat. Sci. Rev 19 (14-15), 1367–1389.
Stroup, D.F., Bohnenstiehl, D.R., Tolstoy, M., Waldhauser, F., Weekly, R.T., 2007. Pulse of the seafloor: Tidal triggering of microearthquakes at 9°50'N East Pacific Rise. Geophys. Res. Lett. 34, L15301.
Sykes, L.R., 1978. Intraplate seismicity, reactivation of preexisting zones of weakness, alkaline magmatism, and other tectonism postdating continental fragmentation. Rev. Geophys. 16 (4), 621–688.
Talbot, C.J., 1999. Ice ages and nuclear waste isolation. Engineering. Geology 52 (3-4), 177–192.
Talwani, P., Acree, S., 1985. Pore pressure diffusion and the mechanism of reservoir-induced seismicity. Pure and Applied Geophysics 122 (6), 947–965.
Tan, Y.J., Tolstoy, M., Waldhauser, F., Bohnenstiehl, D.R., 2018. Tidal triggering of microearthquakes over an eruption cycle at 9°50'N East Pacific Rise. Geophys. Res. Lett. 45 (4), 1825–1831.
Thatcher, W., 2007. Microplate model for the present-day deformation of Tibet. J. Geophys. Res. Solid Earth. 112, B01401.
Thomas, A.M., Nadeau, R.M., Bürgmann, R., 2009. Tremor-tide correlations and near lithostatic pore pressure on the deep San Andreas fault. Nature 462 (7276), 1048–1051.
Thomas, A.M., Bürgmann, R., Shelly, D.R., Beeler, N.M., Rudolph, M.L., 2012. Tidal triggering of low frequency earthquakes near Parkfield, California: Implications for fault mechanics within the brittle-ductile transition. J. Geophys. Res. Solid Earth. 117 (B5), n/a–n/a.
Tiwari, D.K., Jha, B., Kundu, B., Gahalaut, V.K., Vissa, N.K., 2021. Groundwater extraction-induced seismicity around Delhi region. India. Sci. Rep. 11, 10097.
Toksoz, M.N., Kehrer, H.H., 1972. Tectonic strain release by underground nuclear explosions and its effect on seismic discrimination. Geophys. J. R. Astron. Soc. 31 (1-3), 141–161.
van der Elst, N.J., Delorey, A.A., Shelly, D.R., Johnson, P.A., 2016. Fortnightly modulation of San Andreas tremor and low-frequency earthquakes. Proc. Natl. Acad. Sci. U.S.A. 113 (31), 8601–8605.
Vidale, J.E., Agnew, D.C., Johnston, M.J.S., Oppenheimer, D.H., 1998. Absence of earthquake correlation with Earth tides: An indication of high preseismic fault stress rate. J. Geophys. Res. 103 (B10), 24567–24572.
Wahr, J., Khan, S.A., Dam, T., Liu, L., Angelen, J.H., Broeke, M.R., Meertens, C.M., 2013. The use of GPS horizontals for loading studies, with applications to northern California and southeast Greenland. J. Geophys. Res. Solid Earth. 118 (4), 1795–1806.
Wilcock, W.S.D., 2009. Tidal triggering of earthquakes in the Northeast Pacific Ocean. Geophys. J. Int. 179 (2), 1055–1070.
Wu, P., Johnston, P., Lambeck, K., 1999. Postglacial rebound and fault instability in Fennoscandia. Geophysical Journal International 139 (3), 657–670.
Xue, L., Johnson, C.W., Fu, Y., Bürgmann, R., 2020. Seasonal seismicity in the Western Branch of the East African Rift System. Geophys. Res. Lett. 47 (6). https://doi.org/10.1029/2019GL085882.
Yadav, A., Gahalaut, K., Mallika, K., Purnachandra Rao, N., 2015. Annual Periodicity in the Seismicity and Water Levels of the Koyna and Warna Reservoirs, Western India: A Singular Spectrum Analysis. Bull. Seismol. Soc. Am. 105 (1), 464–472.
Yuzariyadi, M., Heki, K., 2021. Enhancement of interplate coupling in adjacent segments after recent megathrust earthquakes. Tectonophys. 801, 228719. https://doi.org/10.1016/j.tecto.2021.228719.
Zatman, S., Gordon, R.G., Richards, M.A., 2001. Analytic models for the dynamics of diffuse oceanic plate boundaries. Geophys. J. Int. 145 (1), 145–156.
Ziv, A., Rubin, A.M., 2000. Static stress transfer and earthquake triggering: No lower threshold in sight? J. Geophys. Res. Solid Earth 105 (B6), 13631–13642.
Zoback, M.D., Moos, D., Mastin, L., Anderson, R.N., 1985. Well bore breakouts and in situ stress. J. Geophys. Res: Solid Earth 90 (B7), 5523–5530.